



Published in final edited form as:

Nat Chem Biol. 2006 May ; 2(5): 265–273.

Chemical modulation of receptor signaling inhibits regenerative angiogenesis in adult zebrafish

Peter E Bayliss^{1,6}, Kimberly L Bellavance^{2,6}, Geoffrey G Whitehead³, Joshua M Abrams², Sandrine Aegerter², Heather S Robbins², Douglas B Cowan⁴, Mark T Keating³, Terence O'Reilly⁵, Jeanette M Wood⁵, Thomas M Roberts¹, and Joanne Chan²

¹Department of Cancer Biology, Dana-Farber Cancer Institute and the Department of Pathology, Harvard Medical School, Boston, Massachusetts 02115, USA.

²Vascular Biology Program, Children's Hospital and the Department of Surgery, Harvard Medical School, Boston, Massachusetts 02115, USA.

³Department of Cardiology, Children's Hospital, Howard Hughes Medical Institute and the Department of Cell Biology, Harvard Medical School, Boston, Massachusetts 02115, USA.

⁴Department of Anesthesia, Harvard Medical School and Children's Hospital, Boston, Massachusetts 02115, USA.

⁵Oncology Research, Novartis Pharma AG, CH-4002 Basel, Switzerland.

Abstract

We examined the role of angiogenesis and the need for receptor signaling using chemical inhibition of the vascular endothelial growth factor receptor in the adult zebrafish tail fin. Using a small-molecule inhibitor, we were able to exert precise control over blood vessel regeneration. An angiogenic limit to tissue regeneration was determined, as avascular tissue containing skin, pigment, neuronal axons and bone precursors could regenerate up to about 1 mm. This indicates that tissues can regenerate without direct interaction with endothelial cells and at a distance from blood supply. We also investigated whether the effects of chemical inhibition could be enhanced in zebrafish vascular mutants. We found that adult zebrafish, heterozygous for a mutation in the critical receptor effector phospholipase C γ 1, show a greater sensitivity to chemical inhibition. This study illustrates the utility of the adult zebrafish as a new model system for receptor signaling and chemical biology.

In the postgenomic era, assigning gene function and delineating signaling pathways require the combined effort of multiple disciplines and approaches. The use of chemical probes has immense potential in examining biological processes and developing specific therapeutic compounds. On the biological side, these goals can be achieved through the appropriate use of model systems. In vitro and cell-based assays have been widely used for drug discovery and chemical library screening¹⁻³. Whole organism approaches are also possible using yeast, worms, flies or zebrafish embryos^{4,5}. Of these, the zebrafish, as a vertebrate organism, has reasonable counterparts to many mammalian organs, tissues and cell types. As such, it affords an opportunity to investigate more complex biological processes⁵. The transparency of the zebrafish embryo has facilitated visual scoring of phenotypic defects. Thus, it has been used extensively for developmental biology and genetics, and in the last few years as a new model

Correspondence should be addressed to J.C. (joanne.chan@childrens.harvard.edu).

⁶These authors contributed equally to this work.

COMPETING INTERESTS STATEMENT The authors declare competing financial interests (see the *Nature Chemical Biology* website for details).

Note: Supplementary information is available on the *Nature Chemical Biology* website.

for chemical biology^{4,5}. However, tissue growth and differentiation are very different in an embryo versus in an adult animal. Embryonic development involves precise coordination of genetic programs that allow the building of a whole organism from a single cell. Therefore, chemical genetic analysis in embryos is dictated by the timing of developmental events. In an adult animal, organ maintenance and cellular needs are different, with turnover and repair being important. Another crucial consideration in developing therapeutics is that many human diseases occur during adulthood. Although a biologically active chemical may act on the same protein(s), the physiological outcome in an embryo could be distinct from its effect in an adult owing to the different needs for target protein function. Thus, testing chemicals in an adult model organism should provide additional insights into their effects on biology.

The adult zebrafish has also been used as a model for regeneration. As in other lower vertebrates, all missing cells and tissues are faithfully replaced in the regenerative process^{6,7}. In contrast, humans and other mammals have limited regenerative capacity, but the mechanisms seem to be conserved. For instance, the *Msx* and *BMP* genes are activated in the regeneration of mammalian digit tips^{8,9}, and during zebrafish caudal fin regeneration¹⁰⁻¹². As the zebrafish is also a genetic model organism, regeneration studies using this model have the potential to reveal important genes and pathways that have been inactivated in mammals^{6,13}.

We chose zebrafish caudal fin regeneration as a model system to examine the role of vascular endothelial growth factor receptor (VEGFR) signaling. The vascular endothelial growth factor (VEGF) ligands and receptors play critical roles in regulating physiological and pathological angiogenesis¹⁴; however, their roles in zebrafish tail fin regeneration have not been investigated. We demonstrated that under the influence of the chemical inhibitor PTK787/ZK222584 (PTK787, 1) (refs. 15,16), regenerative angiogenesis can be separated from tissue regrowth, as a small amount of avascular tissue, up to ~ 1 mm, can be regenerated in the absence of accompanying blood vessels. However, to regenerate beyond this size limit, angiogenesis is required. Using zebrafish genetics, we examined chemical blockade of VEGFR function on adult zebrafish from mutant lines with known recessive embryonic vascular defects. Our study demonstrates a new approach to studying angiogenesis in an adult animal using chemical, molecular and genetic methods. This model system can also provide a platform for evaluating antiangiogenic therapies and discovering biologically active chemical compounds.

RESULTS

Zebrafish caudal fin as a model for regenerative angiogenesis—The zebrafish is a small teleost fish, about 3-4 cm in length and weighing ~ 2 g. It can regenerate many tissues, including the caudal or tail fin, heart and nervous system^{6,17}. Although the zebrafish tail fin is very thin and optically transparent, fin tissues and blood vessels are well defined¹⁸ (Fig. 1). Zebrafish fins are composed of segmented bony fin rays, each comprised of concave, facing hemirays (lepidotrichia)⁶. Vascular architecture in the caudal fin is organized with an artery in the middle of each bony ray, and veins located on either side of the bony structure as described¹⁸ (Fig. 1b,c). A set of smaller blood vessels form the connecting microvasculature in the inter-ray mesenchyme (Fig. 1c,d)¹⁸. Although blood flow can be observed noninvasively by putting an anesthetized zebrafish under a microscope, we have also developed a fluorescent angiography technique to capture an image of perfused vessels (Fig. 1a,c,d; Supplementary Video 1 online shows zebrafish tail fin circulation; also see Methods for detailed procedure).

In fin regeneration experiments, zebrafish caudal fins are amputated at mid-fin level, then allowed to recover. New blood vessels are formed in the regenerated fin shortly after amputation¹⁸. We used angiography in a transgenic zebrafish line in which endothelial cells are labeled with enhanced green fluorescent protein (EGFP; Tg(fli1:EGFP)^{y1})¹⁹, so that an

assessment of endothelial cell growth and migration as well as blood flow could be made simultaneously (Fig. 2). By 3 days post amputation (dpa; compare top and middle panels, Fig. 2), networks of endothelial cells in the regenerated tissue formed a vascular plexus that extended to the fin tip, whereas the corresponding angiography in the same zebrafish tail fin shows that functional blood flow was confined to the proximal region of the regenerated fin¹⁸ (Fig. 2a,b). High-magnification views of the fin tip show an arterial-venous anastomosis at the severed ends of blood vessels to permit blood flow¹⁸ (Fig. 2g), as well as the appearance of endothelial tip cells, novel cells analogous to the neuronal growth cones, which have been proposed to direct vessel migration²⁰ (Fig. 2g,h).

Regenerative angiogenesis is sensitive to chemical inhibition—We tested the small molecule kinase inhibitor PTK787, an anilinothalazine compound that inhibits the human VEGFRs^{15,16}, for its effectiveness in blocking regenerative angiogenesis after caudal fin amputation. This compound has shown high affinity toward the mammalian VEGFRs, VEGFR2 (KDR for the human, or flk-1 for the mouse versions), VEGFR1 (flt-1 for the mouse receptor) and VEGFR3 (flt-4 for the mouse homolog). It can also inhibit the related platelet-derived growth factor (PDGF) and the c-kit receptors at higher concentrations^{15,16,21}. In our previous work using zebrafish embryos, treatment with 5 μ M PTK787 completely prevented the formation of the major blood vessels²². In adult tail fin regeneration, partial inhibition occurred at 100 nM (Fig. 2c,d), and complete inhibition was achieved at 500 nM PTK787 (Fig. 2e,f), approaching nanomolar levels for zebrafish VEGFR2 inhibition in cell culture²². In both embryonic and adult zebrafish assays, we have found potent antiangiogenic effects at the selected inhibitor concentrations where pigmentation, known to be regulated by the c-kit receptor²³, was unaffected²² (shown below). The ability to chemically control adult angiogenesis, either partially or completely inhibiting the process, has provided a useful tool for our study.

The adult fin regenerative angiogenesis assay revealed a ten-fold higher sensitivity to inhibitor levels as compared with the embryonic assay, at 500 nM versus 5 μ M, respectively. Although this enhanced sensitivity could reflect inherent differences between developmental and regenerative angiogenesis, it may also be explained by compound accessibility. The zebrafish caudal fin tip is actually thinner than the embryo at 2 d of development, at \sim 20 μ m versus \sim 200 μ m, respectively. For the adult zebrafish, the drug may also reach the regenerating fin tissue via gill uptake and circulation, a process that might be more efficient than passive diffusion through the embryo²⁴. Although the detailed molecular mechanisms will take some time to define, the practical result is that regenerative angiogenesis in the zebrafish can provide a sensitive read-out for the effectiveness of an antiangiogenic compound.

Our data also show that blood vessels on the proximal side of the amputation site remained predominantly intact and functional during 3 d of treatment post amputation (Fig. 2), suggesting a difference in sensitivity between newly formed versus established vessels. This seems to agree with the goal of antiangiogenic therapy to selectively inhibit highly active, abnormal vessels while leaving quiescent vessels intact. The chemical inhibitor provided facile temporal control over VEGFR function while the zebrafish tail fin model can provide new vessels for examination. To investigate nascent vessel susceptibility, we allowed the fish to recover normally for 5 dpa before chemical inhibition with 500 nM PTK787 for the next 3 d (Supplementary Fig. 1 online). Within the regenerated fin tissue, the distal vessels at the fin tip were most sensitive to VEGFR inhibition (Supplementary Fig. 1c,d online), while proximally located vessels were functional. Thus, within a just a few days of regeneration, changes have taken place for some vessels to become resistant to receptor inhibition, suggesting a reduced dependence on VEGFR signaling.

Molecular analysis of regenerative angiogenesis—In the early stages of caudal fin regeneration, a wound healing epidermis is formed, followed by the dedifferentiation and subsequent proliferation of cells on the proximal side of the cut to form a blastema⁶. Within the blastema, cells are reprogrammed to initiate the coordinated rebuilding of all the cell types required to replace the amputated fin tissue. Several molecular markers have been identified in this process, including the transcription factor *msxb*; the fibroblast growth factor receptor 1, *fgfr1*; as well as the morphogen sonic hedgehog, *shh*^{10-12,25,26}.

We examined the *in situ* RNA expression of the *vegfa* ligand and the *vegfr2* receptor to place these key angiogenic molecules in context with other fin regeneration markers (Fig. 3). We found that the *vegfa* ligand mRNA is detected early on, from about 1 to 1.5 dpa (Fig. 3a,g), whereas the *vegfr2* mRNA, used here as a marker for active endothelial cells, is not detected until 2 dpa (Fig. 3b). At 2 dpa, expression of several other fin regeneration markers, *msxb*, *shh* and *fgfr1*, was detected in control and treated fins (Fig. 3c-f). These data demonstrate that PTK787 is selectively acting on endothelial cells, without affecting genes required for regeneration. As expected, the greatest difference was seen in the *vegfr2* mRNA signal, as the PTK787 inhibitor prevented endothelial cell growth and migration into the newly regenerated tissue (Fig. 3b). Because the *vegfa* and *msxb* genes are both expressed early, we compared their expression at the same stage during fin regeneration (Fig. 3f,g). Sectioning of individual fin rays revealed that cells expressing *vegfa* appear to partially colocalize within a larger *msxb* expression domain. As *msxb* is a marker for blastemal cells at this stage, it seems that a subpopulation of these cells also express the *vegfa* ligand mRNA.

Fin regeneration is limited by angiogenesis—Although the regeneration of a complete fin requires angiogenesis, we have found that in the absence of new blood vessels, limited avascular fin tissue can still be formed (Fig. 4a-f). Within this tissue, skin and pigment cells appeared intact by visual inspection (Fig. 4c). However, the amount of tissue regenerated was limited to ~800 μm at 7 dpa in the presence of PTK787, and remained the same despite increasing the treatment time to 14 d (Fig. 4c,d,g). In washout experiments, when the VEGFR inhibitor was removed after 3 d of treatment, new blood vessels rapidly grew into the regenerated avascular tissue over the next 4 d, implicating persistent expression of angiogenic factors and guidance cues (Fig. 4e,f). This rapid revascularization suggests that the tissue regeneration process was only temporarily halted until angiogenesis could be resumed (Fig. 4a,e). To examine the process of vessel regeneration, we observed the same fish over a time course of several days. In normal regeneration, we observed anastomoses of arteries and veins, plexus formation and vessel remodeling as described¹⁸ (Fig. 4h-j). However, when the fish were first treated with PTK787 for 3 dpa before inhibitor washout and recovery, the amount of plexus formation seemed reduced (Fig. 4i,l).

To investigate the potential role of important angiogenic molecules, we carried out real-time PCR analysis on the regenerated fin tissue, targeting the expression of the *vegfa* ligand and its receptors *vegfr1* and *vegfr2* (Fig. 4n,o and Supplementary Fig. 2 online). Under the influence of PTK787 treatment for 3 dpa, as endothelial cell growth was inhibited, the *vegfa* mRNA levels were markedly increased in the avascular regenerate, at over five-fold higher levels than in control fins where natural regeneration occurred (Fig. 4o). At the same time point, very low levels of the *vegfr2* mRNA were expressed (Fig. 4o), as expected from our *in situ* data (Fig. 3). In these experiments, the inhibitor was removed at 3 dpa and fish were allowed to recover over the next 2 d. In days 4 and 5, as endothelial cells were no longer inhibited, *vegfr2* mRNA expression increased to approach levels in normal regeneration. At the same time, *vegfa* ligand expression was reduced as soon as the VEGFR inhibitor was removed and endothelial cells were allowed to respond. These results demonstrate classical ligand-receptor responses in a living adult animal over the course of a few days that have been revealed using a chemical probe. The expression level of *vegfr1* is very low in comparison with *vegfr2*, even in normal

regeneration, suggesting that VEGFR2 is the major receptor mediating fin regenerative angiogenesis. We also confirmed the expression of *ephrinB2a* and *semaphorin3aa* mRNAs, both during normal regeneration, and in the avascular tissue under chemical inhibition, implicating a role for these guidance molecules during fin regeneration (Supplementary Fig. 2 online).

To examine cell types that can be formed in the fin while blood vessels are inhibited, we used angiography and immunohistochemistry (Fig. 5a-f). The monoclonal antibodies zn-12, for the L2/HNK antigen found on neuronal axons²⁷, or zns-5, for an unknown antigen on scleroblasts or bone-forming cells²⁸, were used to examine the regeneration of nerves or bone tissue in the presence or absence of the antiangiogenic compound. Although the amount of tissue regenerated was reduced when vessels were completely inhibited by PTK787, axonal outgrowth and the regeneration of bone tissue proceeded in a manner similar to the vascularized controls (Fig. 5b,d,f). The use of a chemical probe has revealed that angiogenesis can be uncoupled from nerve and bone regeneration. An active role for endothelial cells has been demonstrated in the adult liver, as sinusoidal endothelial cells provide hepatocyte growth factor to neighboring hepatocytes to promote liver growth²⁹. Although endothelial cells are not required for the initial stages of zebrafish fin regeneration, they may play an important role in the subsequent reorganization of all fin tissues in order to recapitulate the normal tail fin architecture.

In addition to fin tissues and cell types, we also determined whether zebrafish fin vessels are associated with perivascular cells (also known as mural cells, vascular smooth muscle cells or pericytes) as in mammalian vessels³⁰. First we examined the fin vessel ultrastructure using transmission electron microscopy. At the midpoint in the tail fin, the central artery lumen is quite large, with several endothelial cells lining the vessel lumen. With tight junctions between the endothelial cells and the presence of a pericyte, the architecture of a zebrafish tail fin vessel closely resembles that of mammalian blood vessels (Fig. 5g). To determine the extent of pericyte coverage, we tested several known pericyte markers and developed a protocol using a monoclonal antibody to vascular smooth muscle actin, clone B-4 (Fig. 5h). Zebrafish caudal fin vessels exhibit extensive smooth muscle actin staining along the whole length of the fin artery, with less staining in the veins, correlating with the degree of pericyte coverage found in mammalian vessels³¹ (Fig. 5h). In cross section using a transgenic endothelial-eGFP line, *Tg(fli1:EGFP)^{y1}*, colocalization of the artery with smooth muscle actin staining confirmed the arterial enrichment of pericytes (Fig. 5i-k). Using this antibody, we examined several time points for detection during fin regeneration (Fig. 5l,m). We found that smooth muscle actin staining was not detectable until after ~1 week of recovery post amputation (Fig. 5l). By 14 dpa, the amount of staining was comparable to baseline levels in unclipped fins (Fig. 5m and data not shown). Therefore, as in mammalian systems, smooth muscle actin seems to be a marker for more established pericytes. Our trials with available antibodies against known early pericyte markers such as the chondroitin sulfate proteoglycan NG2, nestin, and PDGF receptor- β (PDGFR- β) did not yield useful results in the zebrafish. Development of reliable pericyte detection reagents and transgenic zebrafish lines with fluorescently labeled perivascular cells would greatly facilitate pericyte-endothelial cell studies in the zebrafish.

Inhibitor effectiveness during zebrafish fin regeneration—In considering VEGFR inhibitors, we also examined several other available small molecule kinase inhibitors for comparison with PTK787. The indolinone compound, SU5416 (2), has high affinity for the VEGFRs but also exhibits similar affinities for related receptors (for example, for VEGFR2, IC₅₀ is 220 nM; for PDGFR- β , IC₅₀ is 68 nM; ref.²¹). PTK787 exhibits higher selectivity for the VEGFR family than the PDGFR- β receptor (for example, for VEGFR2, IC₅₀ is 42 nM; for PDGFR- β , IC₅₀ is 490 nM; ref.²¹). For embryonic angiogenesis, our data agreed with a previous report³² (data not shown) showing that SU5416 effectively prevents blood vessel

formation in the zebrafish embryo. In the adult fin, however, we observed tissue growth, but regenerative angiogenesis occurred in a manner similar to controls (Fig. 6a-c). A related indolinone compound, SU11652 (ref. 33) (3), provided an intermediate level of vessel inhibition at low concentrations (Fig. 6d-f). In contrast, AAL993/ZK260255 (AAL993, 4), a compound identified through structural similarity to PTK787 (ref. 21), also inhibited angiogenesis in a similar fashion (Fig. 6g-i).

Differences in biology and chemistry might explain these observations. A recent study took an unbiased approach to examine the affinities of 20 small molecule protein kinase inhibitors against 119 protein kinases³⁴. PTK787 was one of the most selective, targeting only four kinases in addition to VEGFR2. Although SU5416 was not tested, another related indolinone, SU11248, bound 73 additional kinases³⁴. In addition, biological differences between embryonic and adult endothelial cells may be a contributing factor as heterogeneity in vascular beds is well documented^{35,36}. Embryonic endothelial cells might be more susceptible to a broad-spectrum inhibitor if more kinases are required for proper vascular development. In contrast, adult angiogenesis in the tail fin might rely more heavily on VEGFR signaling so that a selective compound such as PTK787 is able to effectively block regenerative angiogenesis without adversely affecting other tissues. These differences also highlight the importance of having both embryonic and adult model systems for vascular biology studies.

VEGFR inhibition in zebrafish mutant lines—As an established genetic model organism, zebrafish mutant lines are available. We examined chemical inhibition of regenerative angiogenesis in three mutant lines known to exhibit homozygous recessive embryonic vascular defects: the *y10* line, which harbors a mutation in an acceptor splice site of the *PLCg1* gene, resulting in deficient gene function³⁷ (*PLCg1^{y10}*); the *gridlock* line, which is due to a hypomorphic mutation in the *hey2* gene^{38,39} (*gr^{m145}*); and the *cloche* line, which features defects in hematopoietic and vascular development in the homozygous recessive embryo⁴⁰ (*clo^{m39}*), but the affected gene has not been identified. Severe vascular defects in the *y10* and *cloche* homozygotes prevented embryonic survival, but the hypomorphic mutation in the *gridlock* line allows some survival to adulthood⁴¹.

To examine differences in vascular response between zebrafish lines, a low concentration of 100 nM PTK787 was chosen for partial inhibition (Fig. 2), so that a further reduction in vascular or tissue regeneration could be measured. To compare regenerative angiogenesis between individuals, adult zebrafish were allowed to recover for 3 dpa with or without the VEGFR inhibitor. At 3 dpa, the amount of tissue versus vessel regeneration was measured for each fish, then expressed as a percentage vascularization (Fig. 7). In the wildtype AB line used throughout this study, this partial VEGFR inhibition routinely generated ~50% vascularization in the newly regenerated tissue (Fig. 7c). We found that heterozygous *PLCg1^{y10/+}* and homozygous *gr^{m145/m145}* adult zebrafish both showed enhanced sensitivity, resulting in ~30% vascularization of regenerated tissue (Fig. 7c). These differences were significant ($P < 0.001$ for both lines compared with wild-type AB line), as determined by our analysis (ANOVA and Tukey test results, **Supplementary Table 1** online). The sensitivity of the *gr^{m145/m145}* and *PLCg1^{y10/+}* adults to PTK787 is correlated with the dependence of both lines on an intact VEGF signaling pathway shown in embryonic studies^{37,41}. Notably, even in the absence of inhibitor, heterozygous *PLCg1^{y10/+}* adults exhibited a significant reduction in vascularization as compared with the other four lines ($P = 0.001$, **Supplementary Table 1** online). In contrast, the *clo^{m39/+}* heterozygous adults responded to the inhibitor in a manner similar to the wild-type AB line, showing ~50% vascularization (Fig. 7c). These results demonstrate the relative sensitivities of two zebrafish mutant lines to VEGFR inhibition, which may reflect their genetic deficiencies.

DISCUSSION

Our study demonstrates chemical regulation of regenerative angiogenesis in the zebrafish caudal fin and establishes the importance of VEGFR signaling in this process. By selectively blocking the angiogenic process, we have uncovered the ability of bone and nerve tissues to regenerate in the absence of adjacent blood vessels. This is the only model in which limited regeneration and tissue differentiation has occurred under chemical inhibition. The assays demonstrate the utility of the zebrafish as a model organism for chemical biology and adult angiogenesis.

Forward and reverse chemical genetics have been used in several model systems. The use of forward chemical genetics in the adult zebrafish is somewhat restricted by the large amount of chemical required and the need for careful visual analysis. Reverse chemical genetics, however, can lead to the rapid dissection of molecular mechanisms and signaling pathways within the complexity of tissues and cell types in the adult. Visualization of each cell type may also be aided by the use of specific transgenic zebrafish lines. The ability to observe distinct cell types within the simple, yet organized, architecture of the zebrafish tail fin provides a unique opportunity to study cell biology *in vivo*. As more tools are being developed and genes identified for zebrafish mutant lines, the use of chemical biology in the zebrafish will expedite studies on signaling pathways and their genetic interactions. Although large-scale chemical library screening is possible in the adult, practical issues must be considered. Despite the higher sensitivity of the adult versus embryonic vascular assays, large volumes are necessary and the need for anesthetization before visual analysis makes automation difficult. However, it may be a very useful second-tier system to evaluate efficacy of compounds that have already shown activity in embryonic zebrafish or other biological assays, to help define chemical specificity and identify adverse effects before investing time and effort on extensive analysis in multiple biological systems.

Our study also revealed an angiogenic limit of about 1 mm during fin regeneration in the presence of VEGFR inhibition. It is possible that this limit is due to hypoxia. Currently, there is a lack of tools to examine hypoxia in the zebrafish. Our attempts to use pimonidazole staining for hypoxia detection did not yield useful results. The detection of the proline hydroxylation state of HIF-1- α as a readout for hypoxia will be facilitated by availability of zebrafish-specific anti-HIF-1- α antibodies.

Our analysis of regenerative angiogenesis in zebrafish mutant lines has revealed an enhanced sensitivity to chemical inhibition in the *PLCg1^{y10}* and *gridlock* lines, correlating with their expression in endothelial cells and their dependence on intact VEGFR signaling during development^{37,39,42}. The *PLCg1* gene is a known effector of mammalian VEGFR2 signaling as shown by biochemical and mouse knock-in studies^{43,44}. It seems to also mediate VEGFR signaling in the zebrafish, as defects in arterial vessel sprouting were observed in *y10* recessive embryos³⁷. Endothelial defects were also observed in *gridlock* homozygous embryos, resulting in artery malformation and blockage of blood flow to the trunk of the embryo^{38,39}. The *gridlock/hey2* gene encodes a basic helix-loop-helix transcriptional repressor expressed in endothelial cells that has been implicated downstream of VEGF and Notch signaling during arterial differentiation⁴². A lower level of *vegfa* expression was detected in *gridlock* homozygotes that can be rescued by overexpression of the ligand, further illustrating a functional relationship between the VEGF pathway and the *gridlock/hey2* gene *in vivo*⁴¹. In our experiments, chemical inhibition of VEGFR signaling, combined with a hypomorphic *gridlock* mutation, might have further reduced the ability of endothelial cells in the caudal fin to grow into the newly regenerated fin.

We also observed that the *cloche* heterozygotes did not exhibit enhanced sensitivity to VEGFR inhibition, showing a response similar to the wild-type line. In the homozygous state, *cloche*

mutant embryos exhibit defects in blood and vessel formation, suggesting a defect in a common progenitor⁴⁰ and gene expression analysis has shown that the affected gene acts upstream of *flk/VEGFR2* (ref. 45). Although our data are consistent with the *cloche* gene acting in a pathway separate from the VEGFR signaling pathway, they are not conclusive. It is possible that the inhibitor dosage used in our assays has not reached the level needed to reveal VEGFR pathway sensitivity in heterozygous *cloche* adults. Our data provide a new approach to studying a receptor signaling pathway in an adult animal using a combination of genetics and chemical biology.

As many human genetic disorders present later in adulthood, we feel that the adult zebrafish system can successfully model these properties. Although the human genome sequence has been completed, the assignment of gene function at the organismal level still imposes an enormous task. With advances in chemical biology and availability of the zebrafish genome on the horizon, this combination can provide a robust model system for investigating the molecular mechanisms underlying human diseases.

METHODS

Maintenance of zebrafish and drug treatments. All animal protocols were approved by the Institutional Animal Care and Use Committees of the Children's Hospital and the Dana-Farber Cancer Institute. Zebrafish were normally maintained at 28.5 °C on a 14 h light/10 h dark cycle in a recirculating tank system. Adult zebrafish tail fins were amputated at mid-fin level. The zebrafish recovered in fish water in controls, or at various concentrations of a kinase inhibitor⁴⁶, in an incubator at 31-33 °C, owing to the faster rates of recovery in wild-type fish⁶. Up to six fish per liter were placed in a tank at one time. The kinase inhibitors PTK787 or AAL993 (Novartis Pharma); SU5416 (Calbiochem, 175580), and SU11652 (Calbiochem, 572660) were dissolved in DMSO at stock concentrations of 2 mM or 5 mM so that the amount of DMSO in the final solution was <0.1%. PTK787 was used at 500 nM for complete inhibition of regenerative angiogenesis or at 100 nM for partial inhibition.

Adult angiography. The adult zebrafish was anesthetized with a standard solution of 0.02% tricaine (w/v; Tricaine Methane Sulfonate, MS-222, Sigma, A5040) for 2-4 min, until the gills stopped moving. The fish was then transferred to a slotted sponge with its ventral side up. A small, longitudinal incision was made just ventral to the gills, over the heart (Fig. 1a). About 5 ml of a fluorescent agent (Molecular Probes) was delivered into the heart using standard microinjection equipment as described³⁸. Fluorescent agents included lectin (Alexa Fluor 488 or 594 conjugates, Molecular Probes L21415 and L21416, respectively), or a 70-kDa dextran (conjugated to Texas Red, used as dye, Molecular Probes, D1864). Sized carboxylate-modified fluorescent microspheres were used only for terminal experiments as shown in **Supplementary Video 1** online (Fluospheres, 4 μm, Molecular Probes, F8858). These reagents were dissolved at 5 mg ml⁻¹ in Danieau's solution (58 mM NaCl, 0.7 mM KCl, 0.4 mM MgSO₄, 0.6 mM Ca (NO₃)₂, 5 mM HEPES, pH 7.6). The fish was placed under a fluorescent microscope (Nikon E600 or Nikon 80i) to assess functional blood vessels in the tail, then immediately placed in a recovery tank. The entire procedure took 5-10 min with nearly all zebrafish recovering within 2-3 min.

Fin vascularization measurements and microscopy. Fin regeneration measurements were taken only when each fin ray was responding consistently to treatment. As the fin rays curved toward the midline, we found rays 2, 3, 4 and 5 from the edges of the caudal fin, to provide the most consistent growth and vascularization. The second ray from the dorsal edge of the fin was used for measurement using the SPOT camera and software (Diagnostic Instruments). The transmission electron micrograph was taken of an adult tail fin at the mid-fin level. The sample was fixed and sectioned using standard methods⁴⁷. Sections (60 nm) were cut with a Reichert Ultracut-Sultramicrotome and mounted on copper grids (200 mesh) by the Harvard Medical

School Electron Microscopy Facility (Boston). Images of endothelial tip cells were acquired with a multi-point spinning disk confocal system (Atto) attached to an Axiovert 200M microscope (Zeiss) using MetaMorph 6.2 software (Universal Imaging).

In situ hybridization. Whole-mount zebrafish fin *in situ* hybridization using various digoxigenin-labeled antisense RNA probes was done using standard methods as described⁴⁸. RNA probes containing digoxigenin-11-UTP (Roche) were visualized using the BM purple alkaline phosphatase substrate (Roche). Selected fins were frozen in OCT compound (Tissue-Tek) and sectioned on a Leica CM3050S cryostat microtome at 20 μ m.

Total RNA extraction, reverse transcription and real-time PCR. We extracted total RNA after homogenization of fins in Trizol (Gibco/Invitrogen) and generated cDNA using the reverse transcription system from Promega with random hexamers according to the manufacturer's procedure. For real-time PCR we used the qPCR SYBR Green Mastermix Plus (Eurogentec) My-IQ one color real-time PCR detection and My-IQ cycler software systems (Bio-Rad). We did the reactions in triplicate.

Primer sequences are reported in **Supplementary Table 2** online. We designed all the primers on exon boundaries to avoid genomic amplification and carried out a fusion curve to check the specificity of each amplification reaction. We standardized all mRNA amounts to the zebrafish b-actin transcript. We carried out Student t-tests to test the difference between clipped (control and PTK treated) and unclipped fins.

Immunostaining. Clipped zebrafish fins were fixed in Dent's fixative (80% methanol, 20% DMSO, v/v) overnight at 4 °C, then stained with the following antibodies: zn-12, zns-5 (Developmental Studies Hybridoma Bank, University of Iowa), or B-4 (Lab Vision, ms-1297-p1), for visualization of axons, bone precursors or smooth muscle actin, respectively. The samples were dehydrated through a methanol series, and re-fixed in 4% (w/v) paraformaldehyde for 2-24 h. The fins were rinsed in phosphate buffered saline (PBS), permeabilized for 20 min in acetone at -20 °C, rinsed twice with PBS and incubated in blocking serum for 1 h at 37 °C, and incubated with 1:50 to 1:200 dilutions of a primary antibody in blocking serum overnight at 4 °C. Samples were washed extensively in PBS, then incubated with a 1:200 dilution of the cy2- or cy3-conjugated secondary antibodies (Jackson Laboratories).

Analysis of zebrafish mutant line sensitivity to chemical inhibition. Caudal fins from adult zebrafish of wild-type or mutant lines were amputated at mid-fin level, then allowed to recover in fish water or in 100 nM PTK787 for partial angiogenic inhibition for 3 dpa as described above. Tissue regrowth and vessel regeneration were measured for each individual as before and expressed as a percentage of vascularization. Statistical analysis was done to determine between group significances using ANOVA and Tukey tests as described (**Supplementary Table 1** online).

Supplementary Material

Refer to Web version on PubMed Central for supplementary material.

ACKNOWLEDGMENTS

We thank J. Folkman, N. Lawson, R. Peterson, J. Mably, F. Serluca, G. Naumov and C. Barnes for helpful discussions and/or critical reading of the manuscript. We acknowledge M. Lin and R. Bolcome for technical assistance with zebrafish care and maintenance and K. Johnson for help with graphics. We thank L. Trakimas for electron microscopy work. This work was supported in part by sponsored research agreements from Novartis to T.M.R. and J.C. and by an award from the Sidney Kimmel Foundation for Cancer Research to J.C. J.C. is a Kimmel Cancer Scholar.

References

1. Chanda SK. Fulfilling the promise: drug discovery in the post-genomic era. *Drug Discov. Today* 2003;8:168–174. [PubMed: 12581711]
2. Drews J. Drug discovery: a historical perspective. *Science* 2000;287:1960–1964. [PubMed: 10720314]
3. Lenz GR. Chemical ligands, genomics, and drug discovery. *Drug Discov. Today* 2000;5:145–156. [PubMed: 10729820]
4. Peterson RT, Link BA, Dowling JE, Schreiber SL. Small molecule developmental screens reveal the logic and timing of vertebrate development. *Proc. Natl. Acad. Sci. USA* 2000;97:12965–12969. [PubMed: 11087852]
5. Zon LI, Peterson RT. In vivo drug discovery in the zebrafish. *Nat. Rev. Drug Discov* 2005;4:35–44. [PubMed: 15688071]
6. Poss KD, Keating MT, Nechiporuk A. Tales of regeneration in zebrafish. *Dev. Dyn* 2003;226:202–210. [PubMed: 12557199]
7. Akimenko MA, Mari-Beffa M, Becerra J, Geraudie J. Old questions, new tools, and some answers to the mystery of fin regeneration. *Dev. Dyn* 2003;226:190–201. [PubMed: 12557198]
8. Reginelli AD, Wang YQ, Sassoon D, Muneoka K. Digit tip regeneration correlates with regions of *Msx1* (*Hox 7*) expression in fetal and newborn mice. *Development* 1995;121:1065–1076. [PubMed: 7538067]
9. Han M, Yang X, Farrington JE, Muneoka K. Digit regeneration is regulated by *Msx1* and *BMP4* in fetal mice. *Development* 2003;130:5123–5132. [PubMed: 12944425]
10. Akimenko MA, Johnson SL, Westerfield M, Ekker M. Differential induction of four *msx* homeobox genes during fin development and regeneration in zebrafish. *Development* 1995;121:347–357. [PubMed: 7768177]
11. Laforest L, et al. Involvement of the sonic hedgehog, *patched 1* and *bmp2* genes in patterning of the zebrafish dermal fin rays. *Development* 1998;125:4175–4184. [PubMed: 9753672]
12. Nechiporuk A, Keating MT. A proliferation gradient between proximal and *msxb*-expressing distal blastema directs zebrafish fin regeneration. *Development* 2002;129:2607–2617. [PubMed: 12015289]
13. Keating MT. Genetic approaches to disease and regeneration. *Phil. Trans. R. Soc. Lond. B* 2004;359:795–798. [PubMed: 15293807]
14. Ferrara N, Gerber HP, LeCouter J. The biology of VEGF and its receptors. *Nat. Med* 2003;9:669–676. [PubMed: 12778165]
15. Bold G, et al. New anilinophthalazines as potent and orally well absorbed inhibitors of the VEGF receptor tyrosine kinases useful as antagonists of tumor-driven angiogenesis. *J. Med. Chem* 2000;43:2310–2323. [PubMed: 10882357]
16. Wood JM, et al. PTK787/ZK 222584, a novel and potent inhibitor of vascular endothelial growth factor receptor tyrosine kinases, impairs vascular endothelial growth factor-induced responses and tumor growth after oral administration. *Cancer Res* 2000;60:2178–2189. [PubMed: 10786682]
17. Poss KD, Wilson LG, Keating MT. Heart regeneration in zebrafish. *Science* 2002;298:2188–2190. [PubMed: 12481136]
18. Huang CC, Lawson ND, Weinstein BM, Johnson SL. *reg6* is required for branching morphogenesis during blood vessel regeneration in zebrafish caudal fins. *Dev. Biol* 2003;264:263–274. [PubMed: 14623247]
19. Lawson N, Weinstein B. In vivo imaging of embryonic vascular development using transgenic zebrafish. *Dev. Biol* 2002;248:307–318. [PubMed: 12167406]
20. Gerhardt H, et al. VEGF guides angiogenic sprouting utilizing endothelial tip cell filopodia. *J. Cell Biol* 2003;161:1163–1177. [PubMed: 12810700]
21. Manley PW, et al. Advances in the structural biology, design and clinical development of VEGF-R kinase inhibitors for the treatment of angiogenesis. *Biochim. Biophys. Acta* 2004;1697:17–27. [PubMed: 15023347]
22. Chan J, Bayliss PE, Wood JM, Roberts TM. Dissection of angiogenic signaling in zebrafish using a chemical genetic approach. *Cancer Cell* 2002;1:257–267. [PubMed: 12086862]

23. Parichy DM, Rawls JF, Pratt SJ, Whitfield TT, Johnson SL. Zebrafish sparse corresponds to an orthologue of c-kit and is required for the morphogenesis of a subpopulation of melanocytes, but is not essential for hematopoiesis or primordial germ cell development. *Development* 1999;126:3425–3436. [PubMed: 10393121]
24. McKim J, Schmieler P, Veith G. Absorption dynamics of organic chemical transport across trout gills as related to octanol-water partition coefficient. *Toxicol. Appl. Pharmacol* 1985;77:1–10. [PubMed: 3966233]
25. Poss KD, et al. Roles for Fgf signaling during zebrafish fin regeneration. *Dev. Biol* 2000;222:347–358. [PubMed: 10837124]
26. Quint E, et al. Bone patterning is altered in the regenerating zebrafish caudal fin after ectopic expression of sonic hedgehog and bmp2b or exposure to cyclopamine. *Proc. Natl. Acad. Sci. USA* 2002;99:8713–8718. [PubMed: 12060710]
27. Metcalfe WK, Myers PZ, Trevarrow B, Bass MB, Kimmel CB. Primary neurons that express the L2/HNK-1 carbohydrate during early development in the zebrafish. *Development* 1990;110:491–504. [PubMed: 1723944]
28. Johnson SL, Weston JA. Temperature-sensitive mutations that cause stage-specific defects in Zebrafish fin regeneration. *Genetics* 1995;141:1583–1595. [PubMed: 8601496]
29. LeCouter J, et al. Angiogenesis-independent endothelial protection of liver: role of VEGFR-1. *Science* 2003;299:890–893. [PubMed: 12574630]
30. Gerhardt H, Betsholtz C. Endothelial-pericyte interactions in angiogenesis. *Cell Tissue Res* 2003;314:15–23. [PubMed: 12883993]
31. Cleaver O, Melton DA. Endothelial signaling during development. *Nat. Med* 2003;9:661–668. [PubMed: 12778164]
32. Cross LM, Cook MA, Lin S, Chen JN, Rubinstein AL. Rapid analysis of angiogenesis drugs in a live fluorescent zebrafish assay. *Arterioscler. Thromb. Vasc. Biol* 2003;23:911–912. [PubMed: 12740225]
33. Liao AT, et al. Inhibition of constitutively active forms of mutant kit by multitargeted indolinone tyrosine kinase inhibitors. *Blood* 2002;100:585–593. [PubMed: 12091352]
34. Fabian MA, et al. A small molecule-kinase interaction map for clinical kinase inhibitors. *Nat. Biotechnol* 2005;23:329–336. [PubMed: 15711537]
35. Arap W, et al. Steps toward mapping the human vasculature by phage display. *Nat. Med* 2002;8:121–127. [PubMed: 11821895]
36. Chi JT, et al. Endothelial cell diversity revealed by global expression profiling. *Proc. Natl. Acad. Sci. USA* 2003;100:10623–10628. [PubMed: 12963823]
37. Lawson ND, Mugford JW, Diamond BA, Weinstein BM. Phospholipase C γ -1 is required downstream of vascular endothelial growth factor during arterial development. *Genes Dev* 2003;17:1346–1351. [PubMed: 12782653]
38. Weinstein BM, Stemple DL, Driever W, Fishman MC. Gridlock, a localized heritable vascular patterning defect in the zebrafish. *Nat. Med* 1995;1:1143–1147. [PubMed: 7584985]
39. Zhong TP. *gridlock*, an HLH gene required for assembly of the aorta in zebrafish. *Science* 2000;287:1820–1824. [PubMed: 10710309]
40. Stainier DY, Weinstein BM, Detrich HW III, Zon LI, Fishman MC. Cloche, an early acting zebrafish gene, is required by both the endothelial and hematopoietic lineages. *Development* 1995;121:3141–3150. [PubMed: 7588049]
41. Peterson RT, et al. Chemical suppression of a genetic mutation in a zebrafish model of aortic coarctation. *Nat. Biotechnol* 2004;22:595–599. [PubMed: 15097998]
42. Zhong TP. Gridlock signalling pathway fashions the first embryonic artery. *Nature* 2001;414:216–220. [PubMed: 11700560]
43. Takahashi T, Yamaguchi S, Chida K, Shibuya M. A single autophosphorylation site on KDR/Flk-1 is essential for *vegf-a*-dependent activation of PLC- γ and DNA synthesis in vascular endothelial cells. *EMBO J* 2001;20:2768–2778. [PubMed: 11387210]
44. Sakurai Y, Ohgimoto K, Kataoka Y, Yoshida N, Shibuya M. Essential role of Flk-1 (VEGF receptor 2) tyrosine residue 1173 in vasculogenesis in mice. *Proc. Natl. Acad. Sci. USA* 2005;102:1076–1081. [PubMed: 15644447]

45. Liao W, et al. The zebrafish gene *cloche* acts upstream of a *flk-1* homologue to regulate endothelial cell differentiation. *Development* 1997;124:381–389. [PubMed: 9053314]
46. Westerfield, M. *The Zebrafish Book: Guide for the Laboratory Use of Zebrafish (Danio rerio)*. Univ. of Oregon Press; Eugene, Oregon, USA: 1995.
47. Morikawa S, et al. Abnormalities in pericytes on blood vessels and endothelial sprouts in tumors. *Am. J. Pathol* 2002;160:985–1000. [PubMed: 11891196]
48. Chan J, et al. Morphogenesis of prechordal plate and notochord requires intact Eph/ephrin B signaling. *Dev. Biol* 2001;234:470–482. [PubMed: 11397014]

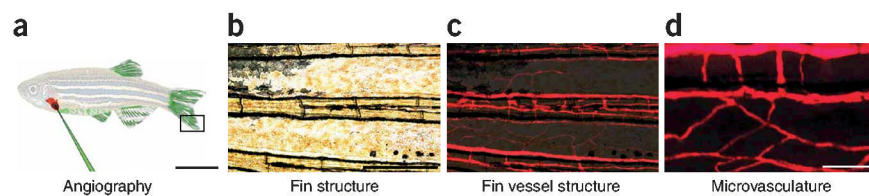


Figure 1. Zebrafish tail fin vasculature and ease of adult angiography. **(a)** Schematic diagram showing the location of the adult zebrafish heart for intracardiac injection and adult angiography. A fluorescent agent microinjected through the heart circulates throughout the fish and is visible in all the fins within minutes. **(b,c)** Enlarged views of the same tail fin region. **(b)** Pigment and bony structures of the fin ray in bright field. **(c)** Blood vessels after fluorescent angiography. **(d)** Magnified region in c of connecting blood vessels of the fin microvasculature. Scale bars, 1 cm **(a)**; 500 μm **(b,c)**; 100 μm **(d)**.

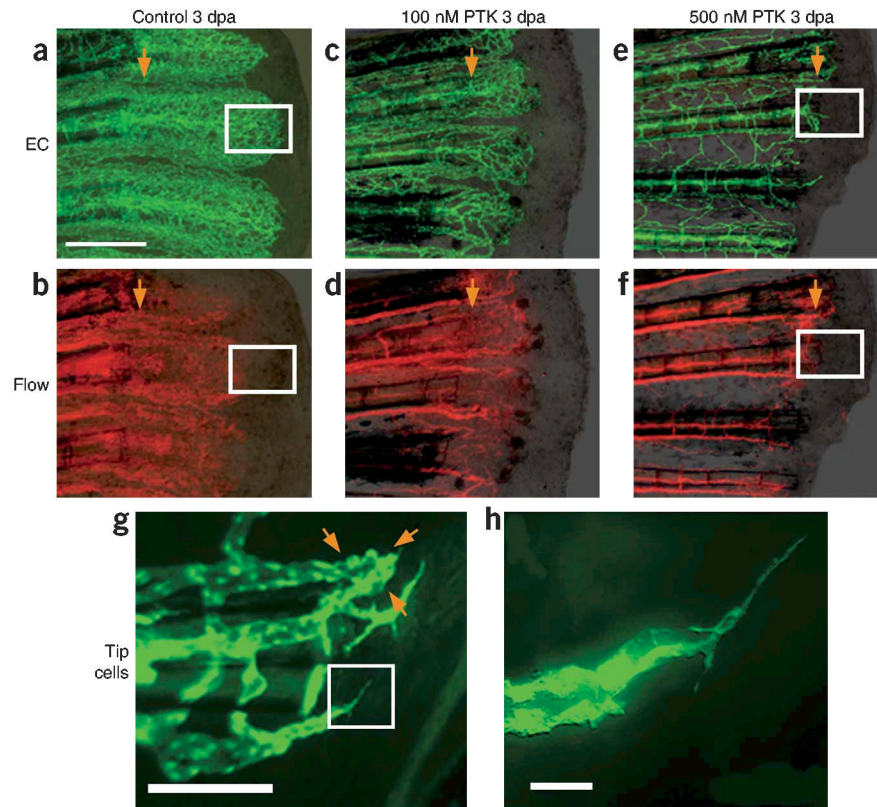


Figure 2.

Tail fin vessel regeneration is sensitive to VEGFR inhibition. Top panels, endothelial cells (EC, green) using a transgenic endothelial-eGFP line, $Tg(fli1:EGFP)^{y1}$. Middle panels, blood flow (Flow, red) using angiography in the same fish. Bottom panels, endothelial tip cells. (a,b) Adult zebrafish tail fins were clipped, then allowed to recover for 3 dpa. (c-f) Fish were treated with PTK787 as indicated. White boxes indicate areas where endothelial cells have not yet formed into perfused blood vessels. (g,h) Filopodia from the endothelial tip cells were found to extend into avascular tissue. Abbreviations for all figures: dpa, days post amputation; EC, endothelial cells; Flow indicates angiography. Orange arrow, amputation site for all figures. Scale bars, 500 μm (a-f); 50 μm (g); 10 μm (h).

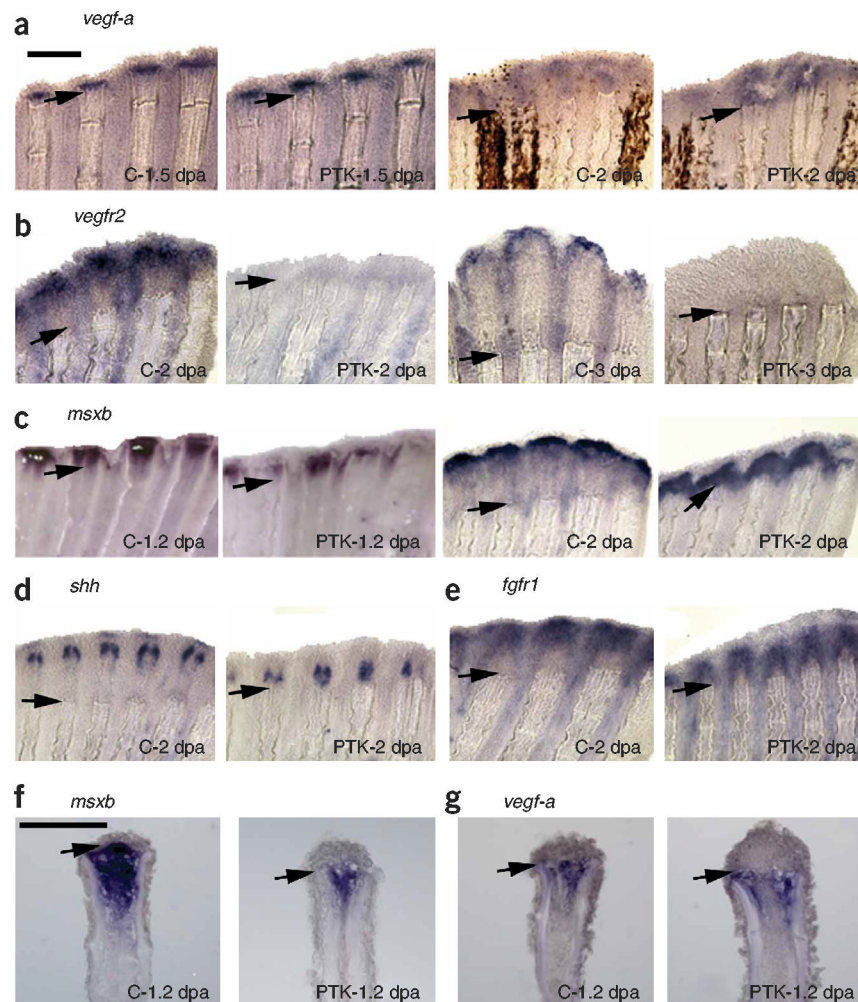


Figure 3. Molecular analysis of regenerative angiogenesis. *In situ* antisense RNA hybridizations with various probes and stages in control (C) or PTK787 (PTK) treated fin samples as indicated. (a-g) *In situ* probes *vegf-a*, *vegfr2*, *msxb*, *shh* or *fgfr1* were used on fin samples as indicated. Black arrows, clip sites in all panels. (f,g) Frozen sections of 1.2 dpa fins showing location of *msxb* and *vegf-a* mRNA staining. Scale bars, 500 μm (a-e), and 50 μm (f,g).

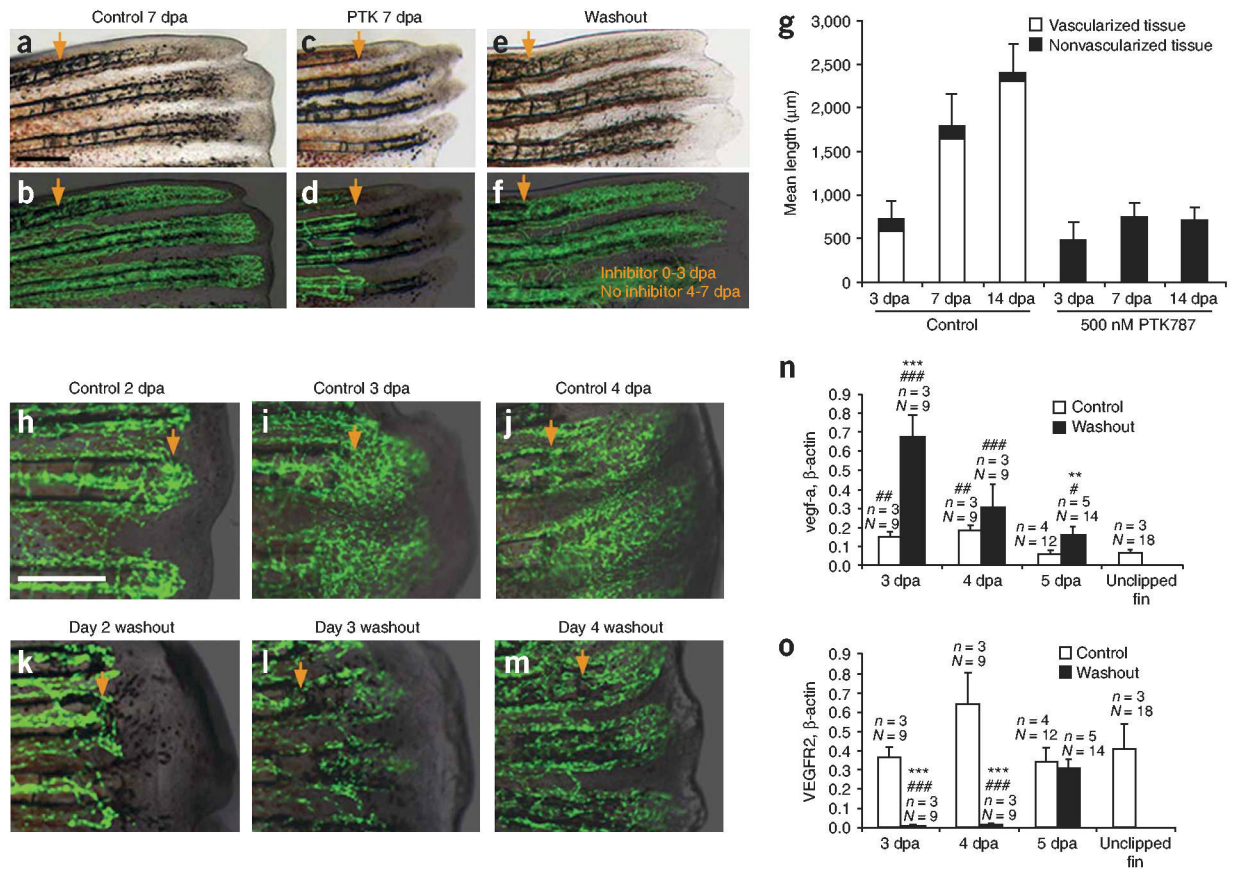


Figure 4. Caudal fin regrowth is limited by angiogenesis. **(a-f)** The same fins are shown in bright field (top panels) and with the corresponding endothelial-eGFP signal (bottom panels). Zebrafish tail fins were clipped, then allowed to recover normally or treated with PTK787 inhibitor as indicated. **(g)** Quantitative comparison of vessel and fin regeneration in control and PTK787-treated fish. Black bars, nonvascularized fin tissue; white bars, vascularized tissue. Average values are plotted for fin and vessel growth ($n = 15$). **(h-m)** Time-course analysis of fin recovery in control (top panels) or PTK787-treated endothelial-eGFP fish (bottom panels) in washout experiment. **(n,o)** Changes in *vegf-a* **(n)** or *vegfr2* **(o)** mRNA levels standardized to β -actin during caudal fin regeneration in control (white bars) or washout where PTK787 was removed at 3 dpa (black bars). Gray bars, levels in unclipped fins. n , number of experimental replicates (pool of fins); N , number of fins used; *, significantly different from control (*, $P \leq 0.01$; ***, $P \leq 0.001$); #, significantly different from unclipped fin (#, $P \leq 0.05$; ##, $P \leq 0.01$; ###, $P \leq 0.001$). Error bars indicate s.d. Scale bars, 500 μ m.

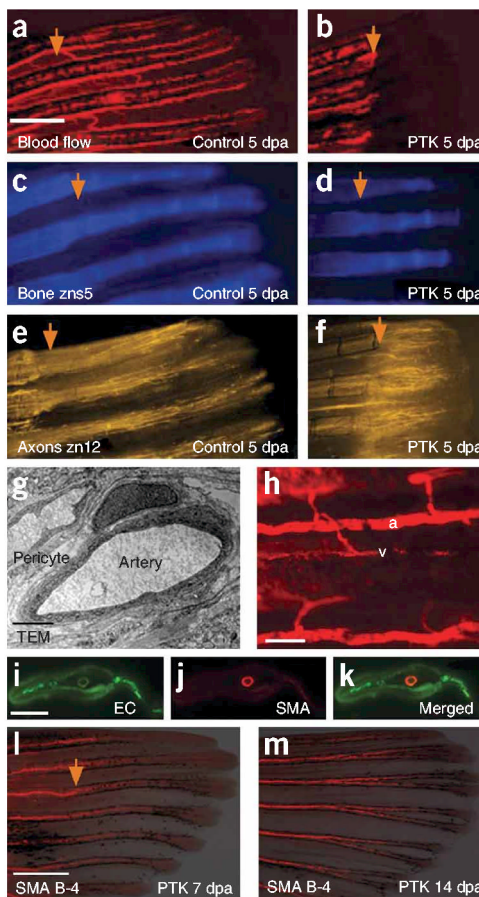


Figure 5. Examination of tissues and cell types in the zebrafish tail fin. **(a-f)** Zebrafish tail fins were clipped and allowed to recover with or without PTK787 as indicated. In the presence of PTK787, regenerative angiogenesis is prevented as indicated by angiography in a,b. Monoclonal antibodies zns-5 or zn-12 were used to examine bone or nerve staining in c,d or e,f, respectively. Regeneration of both tissue types appears unaffected by PTK787 **(d,f)**. **(g)** Transmission electron micrograph (TEM) of the caudal fin at mid-fin level. A central artery (artery) and a perivascular cell (pericyte) are indicated. **(h)** Higher magnification of tail fin vessels stained for smooth muscle actin using the monoclonal antibody B-4. An artery is labeled ‘a’ and a vein is labeled ‘v.’ **(i-k)** Frozen cross-section of a caudal fin at mid-fin level using endothelial-eGFP (EC) and smooth muscle actin (SMA) in the same sample. **(l-m)** Antibody staining for smooth muscle actin in 7 dpa or 14 dpa adult fins using monoclonal antibody B-4. Orange arrow, clip site in l; clip site is outside the image in m, due to the large amount of regrown tissue. Scale bars, 500 μm **(a-f,l)**; 5 μm **(g)**; 10 μm **(h)**; 50 μm **(i-k)**.

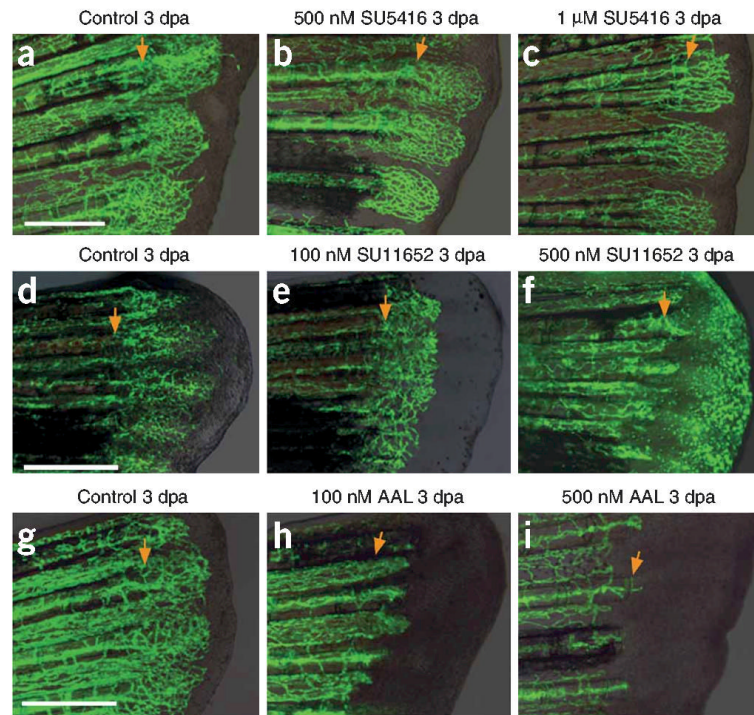


Figure 6. Effectiveness of chemical inhibitors on regenerative angiogenesis. Adult zebrafish tail fins were clipped, then allowed to recover for 3 dpa under control conditions or with inhibitors as indicated. SU5416 (**a-c**), SU11652 (**d-f**) or AAL993 (AAL; **g-i**).

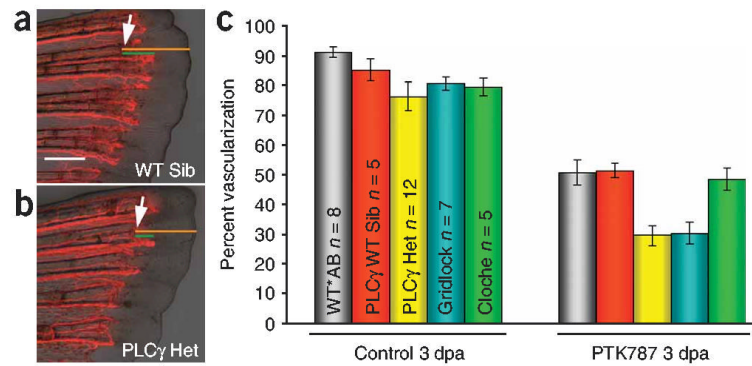


Figure 7.

Chemical analysis of regenerative angiogenesis in zebrafish lines. (a,b) Zebrafish tail fins from heterozygous PLCg1^{y10/+} adults (PLC γ Het; b) and their age-matched wild-type siblings (PLCg1^{+/+}; WT Sib; a) were clipped and allowed to recover for 3 d in 100 nM PTK787 for partial inhibition. White arrow, clip site; orange line, total amount of tissue regrowth; green line, amount of vascularization in the regenerated tissue. (c) Tissue regeneration and the percentage of vascularization at 3 dpa were determined in zebrafish lines in controls (Control 3 dpa) or with PTK787 treatment (PTK787 3 dpa) as indicated. For each line, the sample numbers are the same for control or for inhibitor treatment: wild-type AB strain (n = 8); PLCg1^{+/+} wild-type siblings (n = 5); PLCg1^{y10/+} heterozygous adults (n = 12); homozygous grl^{m145/m145} adults (n = 5). Error bars indicate s.d. (n = 7); heterozygous clo^{m39/+} adults Scale bar, 500 μm (a,b).